

Revised modelling of the post-AD 79 volcanic deposits of Somma-Vesuvius to reconstruct the pre-AD 79 topography of the Sarno River plain (Italy)

SEBASTIAN VOGEL^{1,3*}, MICHAEL MÄRKER^{1,2} and FLORIAN SEILER³

¹Heidelberg Academy of Sciences and Humanities c/o University of Tübingen, Rümelinstraße 19-23, D-72070 Tübingen, Germany;
* sv@dainst.de

²Department of Vegetation, Soil, Environment and Agroforestry Sciences, University of Florence, P.zza S. Marco 4, I-50121 Florence, Italy

³German Archaeological Institute, Germany, Podbielskiallee 69-71, D-14195 Berlin, Germany

(Manuscript received May 10, 2010; accepted in revised form November 16, 2010)

Abstract: In this study the methodology proposed by Vogel & Märker (2010) to reconstruct the pre-AD 79 topography and paleo-environmental features of the Sarno River plain (Italy) was considerably revised and improved. The methodology is based on an extensive dataset of stratigraphical information from the entire Sarno River plain, a high-resolution present-day digital elevation model (DEM) and a classification and regression tree approach. The dataset was re-evaluated and 32 additional stratigraphical drillings were collected in areas that were not or insufficiently covered by previous stratigraphic data. Altogether, an assemblage of 1,840 drillings, containing information about the depth from the present-day surface to the pre-AD 79 paleo-surface (thickness of post-AD 79 deposits) and the character of the pre-AD 79 paleo-layer of the Sarno River plain was utilized. Moreover, an improved preprocessing of the input parameters attained a distinct progress in model performance in comparison to the previous model of Vogel & Märker (2010). Subsequently, a spatial model of the post-AD 79 deposits was generated. The modelled deposits were then used to reconstruct the pre-AD 79 topography of the Sarno River plain. Moreover, paleo-environmental and paleo-geomorphological features such as the paleo-coastline, the paleo-Sarno River and its floodplain, alluvial fans near the Tyrrhenian coast as well as abrasion terraces of historical and protohistorical coastlines were identified. This reconstruction represents a qualitative improvement of the previous work by Vogel & Märker (2010).

Key words: AD 79, Sarno River plain, Somma-Vesuvius, modelling, paleo-environment, paleo-topography, landscape reconstruction.

Introduction

When the Somma-Vesuvius volcanic complex explosively erupted AD 79 its adjacent south-eastern territory was covered by volcanic deposits of some meters thickness in a very short period of time. Consequently, not only the Roman settlements of Pompeii and Herculaneum but also almost the entire ancient landscape of the Sarno River plain were buried and thereby preserved to a certain extent. Since the laterally extensive volcanic deposits of AD 79 show a specific and therefore readily identifiable stratigraphy they can be used as a chronostratigraphic marker. This stratigraphy consists of white phonolitic and grey tephritic phonolitic pumice lapilli fallout on top of the pre-AD 79 Roman surface. The grey pumice is interrupted and overlain by several ash layers of pyroclastic surge and flow deposits (Sigurdsson et al. 1985; Carey & Sigurdsson 1987; Civetta et al. 1991; Cioni et al. 1992; Lirer et al. 1993; Luongo et al. 2003).

Vogel & Märker (2010) made a detailed review of past paleo-environmental studies in the Sarno River plain including Cinque & Russo (1986), Livadie et al. (1990), Furnari (1994), Pescatore et al. (1999), Di Maio & Pagano (2003) and Stefani & Di Maio (2003). These studies mostly focussed on the delineation of the coastline before AD 79 and the paleo-course of the Sarno River and its estuary mouth. Vogel & Märker

(2010) demonstrated that the pre-AD 79 paleo-surface of the entire Sarno River plain can be reconstructed by using sophisticated geostatistical methods. This methodology is based on an extensive dataset of stratigraphical information, a high-resolution present-day digital elevation model (DEM) and a classification and regression tree approach.

The objective of this paper is to revise and improve the spatial model of post-AD 79 deposits established by Vogel & Märker (2010) as well as the deduced pre-AD 79 paleo-topography and selected paleo-environmental features by using an increased number of stratigraphical data and further preprocessing the input parameters.

Study area

The Sarno River plain is located south of the volcanic complex of Somma-Vesuvius and belongs to the southern part of the Pliocene-Pleistocene graben structure of the Campanian Plain. It has a surface area of approximately 210 km² and is drained by the Sarno River and its tributaries. In the south and in the east the basin is flanked by the Lattari and Sarno Mountains belonging to the Apennine Mountain chain. In the west it has an approximately 10 km long coastline with the Tyrrhenian Sea. The Sarno River plain consists

of marine, alluvial and volcanic deposits lying on top of a carbonate platform that reaches down to a maximum depth of 2 km b.s.l. (Cella et al. 2007). During the last 25,000 years the Sarno River plain has been repeatedly influenced by the periodic activity of the Somma-Vesuvius volcano. Several explosive (Plinian) eruptions have occurred, each one marking the beginning of a new eruptive cycle after a certain period of quiescence that can last some thousand years (Delibrias et al. 1979; Santacroce 1987; Rolandi et al. 1993a,b; Andronico et al. 1995; Civetta et al. 1998; Sigurdsson 2002; Cella et al. 2007). Among these Plinian eruptions the event of AD 79 was one of the most destructive and today it is one of the most well-known and most studied volcanic eruptions in history.

Methodology

The methodology applied to reconstruct the pre-AD 79 topography of the Sarno River plain was described in detail by Vogel & Märker (2010). Most fundamentally, it is based on an extensive dataset of stratigraphic cross-sections from a total of 1,840 core drillings to gain a representative network of stratigraphical information for the entire Sarno River plain (Fig. 1). The collected core drillings were carried out during construction works, as well as past archaeological and geological studies. Compared to the previous model of Vogel & Märker (2010) 32 additional sections from drillings were collected in the area of Boscoreale, Stabiae, Angri and Longola-Poggio-marino. The new drillings north of Angri, but also in Boscoreale, cover an area where stratigraphical data were so far missing. Additionally, between 2007 and 2009 we conducted 24 further core drillings in areas with insufficient stratigraphical information and included them in the modelling.

A characteristic feature of the AD 79 explosive eruptions of Somma-Vesuvius is a thick layer of white phonolitic pumice that was deposited upon a dark Roman paleosol. Moreover, no former or later eruption of Somma-Vesuvius is comparable with that of AD 79 in terms of magnitude, stratigraphic appearance and spatial distribution. Consequently, the stratigraphic position of the Roman paleo-surface can be easily identified and measured even though some drillings were carried out without strict scientific control but during construction works.

The core drillings were collected, localized and digitized using geographical information systems (GIS). The stratigraphy of the drillings was determined, above all identifying the volcanic deposits of the AD 79 eruption, the pre-AD 79 paleo-surface underneath and measuring the depth from the present-day surface to the pre-AD 79 surface (thickness of post-AD 79 deposits). Furthermore, the pre-AD 79 layer was characterized and categorized distinguishing five different environmental classes which later on allows the reconstruction of some important paleo-environmental features of the Sarno River plain (Vogel & Märker 2010):

(i) Terrestrial deposits

Roman paleosol of loamy sand that is characterized by the formation of a dark humus A horizon and sometimes by an initial A/Bw weathering horizon. It is composed of fine

weathered ash, rounded pumice, lapilli and lithic clasts. Sometimes traces of agricultural use and former vegetation as well as fragments of ceramics can be found.

(ii) Fluvial deposits

Fluvial deposits consist of conglomerates of black fluvial gravel within a sandy or loamy matrix. They contain rounded pumice and lithic clasts mostly sorted in thin layers of different deposition cycles. Sometimes fragments of travertine can also be found. They identify the alluvium of rivers, mainly of the Sarno River network.

(iii) Palustrine deposits

Palustrine deposits consist of loamy substrate interconnected with dark greyish peaty layers rich in organic matter and plant remains. They are often characterized by hydro-morphic features indicating pedogenetic processes of gleyzation that are caused by the presence of a high ground water table. Furthermore they can contain pumice, travertine plates and shells of freshwater gastropods. These deposits represent wetlands (bogs and swamps) that are mainly linked to the floodplain of the Sarno River.

(iv) Littoral deposits

Littoral deposits are associated with the ancient coastline. They contain well-sorted grey littoral gravel and sand with rounded pumice and lithic clasts.

(v) Marine deposits

Marine deposits consist of grey marine gravel and sand that can contain remains of marine organisms (e.g. shells of saltwater gastropods). They indicate the presence of the Tyrrhenian Sea or lagoons that are separated from the active shore by littoral deposits.

Since both, fluvial and palustrine deposits are closely related to the paleo-Sarno River the two classes were finally merged to identify the floodplain of the paleo-Sarno River. If the pre-AD 79 layer could not be clearly related to one of these five classes, additionally, mixed classes were defined to incorporate intermediate forms of deposits.

Our approach is based on the hypothesis that the eruption AD 79 mantled the ancient topography of the Sarno River plain leaving ancient physiographic elements still recognizable in the present-day topography (Sigurdsson & Carey 2002; Stefani & Di Maio 2003; Vogel & Märker 2010). Consequently, the present-day topography can be utilized for reconstructing the ancient conditions. This is supported by Ohlig (2001) who states that the general structure of the Pompeian hill must have remained constant after the eruption of AD 79 apart from a different absolute altitude.

To model the pre-AD 79 topography of the Sarno River plain a classification and regression tree approach was applied using a high-resolution present-day digital elevation model (DEM) and 16 deduced primary and secondary topographic indices. Neotectonic phenomena that occurred before AD 79 are taken into account in this modelling approach because their resulting landforms are incorporated into the present-day topography. However, the present-day DEM can also contain structures of recent neotectonic activities (after AD 79) which may by mistake be transferred to the reconstructed pre-AD 79 topography. By means of the stratigraphical information from the drilling data, such as the

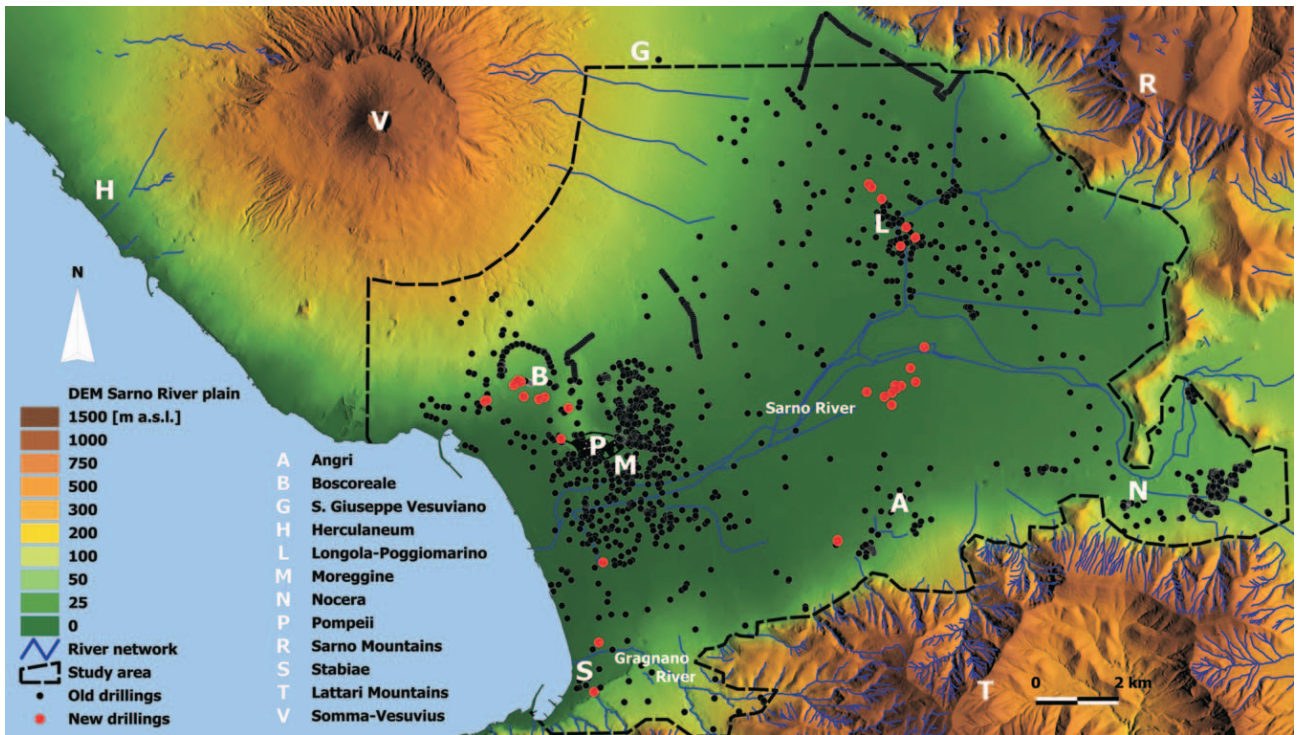


Fig. 1. Present-day digital elevation model (DEM) and fluvial network of the Sarno River plain with the location of 1,840 stratigraphical core drillings. New collected or conducted drillings are indicated in red. Letters mark sites of interest.

elevation of the pre-AD 79 littoral deposits, major elevation discrepancies can be identified.

Classification and regression trees is an algorithm used for exploratory data analysis and predictive modelling to discover features and structural patterns in large databases by determining the correlation between predictor variables and a response variable (Breiman et al. 1984; Myles et al. 2004). For the model generation we used the TreeNet software (Salford Systems). As predictor variables we used the present-day DEM and 16 deduced primary and secondary topographic indices and as the response variable we took the depth to the pre-AD 79 surface (thickness of post-AD 79 deposits) (Table 1).

Table 1: Predictor variables used for the modelling process in TreeNet (Salford Systems).

Predictor variables	Method/Reference
Elevation	Topo to Raster (ArcGIS 9.2)/SIT 1:5,000
Altitude above channel network	SAGA terrain analysis module (Olaya & Conrad 2008)
Analytical hillshading	SAGA terrain analysis module (Olaya & Conrad 2008)
Aspect	SAGA terrain analysis module (Zevenbergen & Thorne 1987)
Catchment area	SAGA terrain analysis module (Olaya & Conrad 2008)
Channel network	SAGA terrain analysis module (Olaya & Conrad 2008)
Channel network base level	SAGA terrain analysis module (Olaya & Conrad 2008)
Convergence index	SAGA terrain analysis module (Köthe & Lehmeier 1993)
Curvature	SAGA terrain analysis module (Zevenbergen & Thorne 1987)
Curvature classification	SAGA terrain analysis module (Dikau 1988)
Plan curvature	SAGA terrain analysis module (Zevenbergen & Thorne 1987)
Profile curvature	SAGA terrain analysis module (Zevenbergen & Thorne 1987)
LS-factor	SAGA terrain analysis module (Olaya & Conrad 2008)
Slope	SAGA terrain analysis module (Zevenbergen & Thorne 1987)
Stream power	SAGA terrain analysis module (Olaya & Conrad 2008)
Watershed subbasins	SAGA terrain analysis module (Olaya & Conrad 2008)
Topographic wetness index	SAGA terrain analysis module (Olaya & Conrad 2008)

Before entering the input parameters into TreeNet the quality of all 1,840 stratigraphical drilling data were re-evaluated. Plausibility checks were carried out on every drilling point by comparison with the surrounding nearest neighbours to identify drillings where the AD 79 volcanic deposits were not correctly determined and by that also the pre-AD 79 paleo-surface. Furthermore, the original drilling documentation was double-checked for drillings whose location was incorrect. By means of a statistical evaluation of the stratigraphical data outliers among the drilling points were detected and eliminated. Moreover, the aspect (A) was transformed according to Beers et al. (1966) following $A' = \cos(45 - A) + 1$. Instead of the common range of the aspect where 0° and 360° represent identical values the aspect was transformed to range of values between 0 and 2. However, it turned out to not significantly improve the model performance. Several preliminary model runs were performed with different presettings, such as number of grown trees and by leaving out different predictor variables. Thus, the sensitivity of a particular predictor variable with respect to the model performance was tested to optimize the prediction.

In order to determine the pre-AD 79 topography of the Sarno River plain the modelled thickness of post-AD 79 deposit was subtracted from the present-day DEM. The pre-AD 79 Sarno River

network was reconstructed by delineation of linear thalweg features of the pre-AD 79 topography using the SAGA terrain analysis module (Olaya & Conrad 2008). The reconstruction of specific paleo-environmental features of the pre-AD 79 surface such as the ancient coastline or the floodplain of the paleo-Sarno River was done by attributing the classified environmental character of the pre-AD 79 paleo-layer to the modelled pre-AD 79 topography (Vogel & Märker 2010).

Results and discussion

The statistical evaluation of the thickness of post-AD 79 deposits of the drilling dataset reveals a range of values between 0 and 19 m (Fig. 2). Drillings having a thickness of more than 19 m can be statistically considered as outliers which apply to 10 of the 1,840 drillings. Disregarding the outliers the arithmetic mean thickness of post-AD 79 deposits is 5.8 m, the median is at 5.3 m and the standard deviation is 3.1 m. Furthermore, 95 % of the drilling data are covering a range between 1.25 and 15 m.

During preliminary model runs the sensitivity test of the predictor variables pointed out that the topographic index 'watershed subbasins' (SAGA terrain analysis module) pro-

duced a lot of artifacts on the regionalized thickness of the post-AD 79 deposits. Consequently, it was left out of the modelling process. Fig. 3 shows the performance of the obtained regression model. The minimum mean absolute error of the training dataset is 0.98 m and that of the test dataset 1.68 m, which is similar to the previous model of Vogel & Märker (2010). 2,094 trees were grown to achieve the smallest test mean absolute error (Fig. 3A). The general model performance of the training and test dataset is illustrated in Fig. 3B and C, respectively. The gain charts show the percentage of population (x-axis) related to the percentage of the target variable (y-axis). The higher the percentage of the target variable with respective low population percentages, the better is the model. In this case the current model performance shows a clear positive correlation similar to the previous model (Vogel & Märker 2010).

The modelled thickness of the post-AD 79 deposits of the Sarno River plain is illustrated in Fig. 4A. It shows a distinct spatial distribution of post-AD 79 deposits ranging from 1.1 to 15.6 m. This range of values corresponds well to the calculated range of 95 % of the drilling data.

Apart from the internal model validation that is performed by TreeNet an external validation of the model results was carried out by comparing the modelled thickness of the post-AD 79

deposits with the real thickness given by the 1,840 drilling data (Fig. 4B). Figure 4B documents an improvement of the new prediction in respect to Vogel & Märker (2010). It shows that 79 % of the drilling points match the modelled thickness with an accuracy of less than 2 m and 50 % of the drilling points with less than 1 m. The respective percentages of the previous model were 44 % and 24 %. The mean thickness of modelled post-AD 79 deposits is 5.6 m (6.5 m in Vogel & Märker 2010) which lies exactly between the arithmetic mean of 5.8 m and the median of 5.3 m obtained from the drilling data. Best agreement between model and drilling data was attained for the plain areas where the post-AD 79 deposits are rather thin. However, with increasing thickness of post-AD 79 deposits and with increasing relief towards the slopes of Somma-Vesuvius and the Apennine Mountains the difference between real and modelled thickness also increases (Fig. 4B).

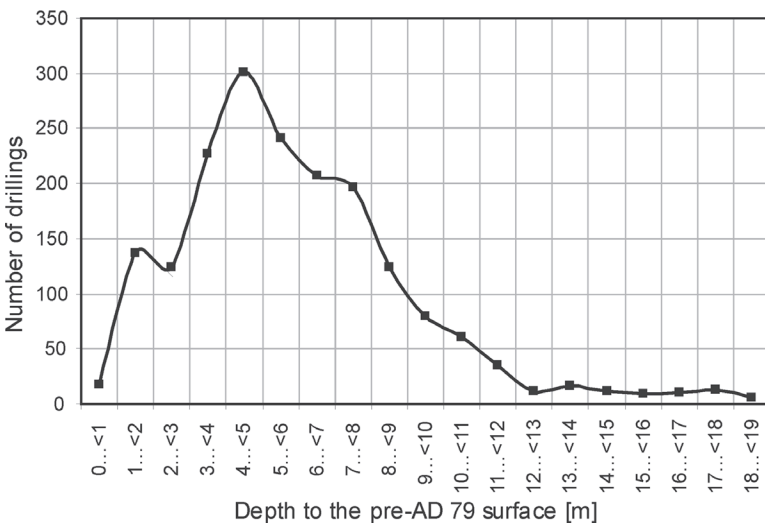


Fig. 2. Histogram of the drilling data regarding the depth to the pre-AD 79 surface.

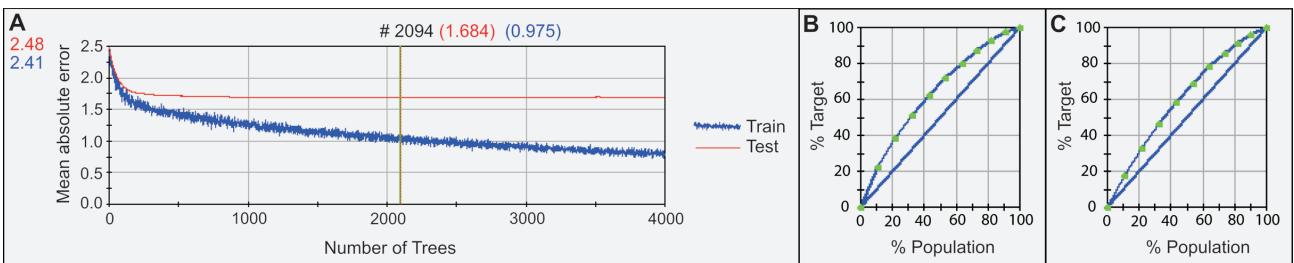


Fig. 3. A — Mean absolute error [m] of the depth to the pre-AD 79 surface versus number of trees of the training and test dataset. The minimum mean absolute error of the training dataset of 0.98 m and of the test dataset of 1.68 m was attained at 2,094 grown trees. B — Gain chart of the training dataset. C — Gain chart of the test dataset (TreeNet).

From 144 drilling points at the northern boundary of the Sarno River plain it turned out that with the present methodology the thickness of post-AD 79 deposits can only be reconstructed northwards up to the modern town of S. Giuseppe Vesuviano (Fig. 1). There the spatial limit of the area of deposition of the AD 79 eruption is reached. Hence,

the volcanic material from the AD 79 eruption is missing in the drilling cores and the pre-AD 79 paleo-surface cannot be clearly identified anymore.

From the modelled depth to the pre-AD 79 surface (Fig. 4A) and the importance of the predictor variables for the model generation (Table 2) it can be observed that the

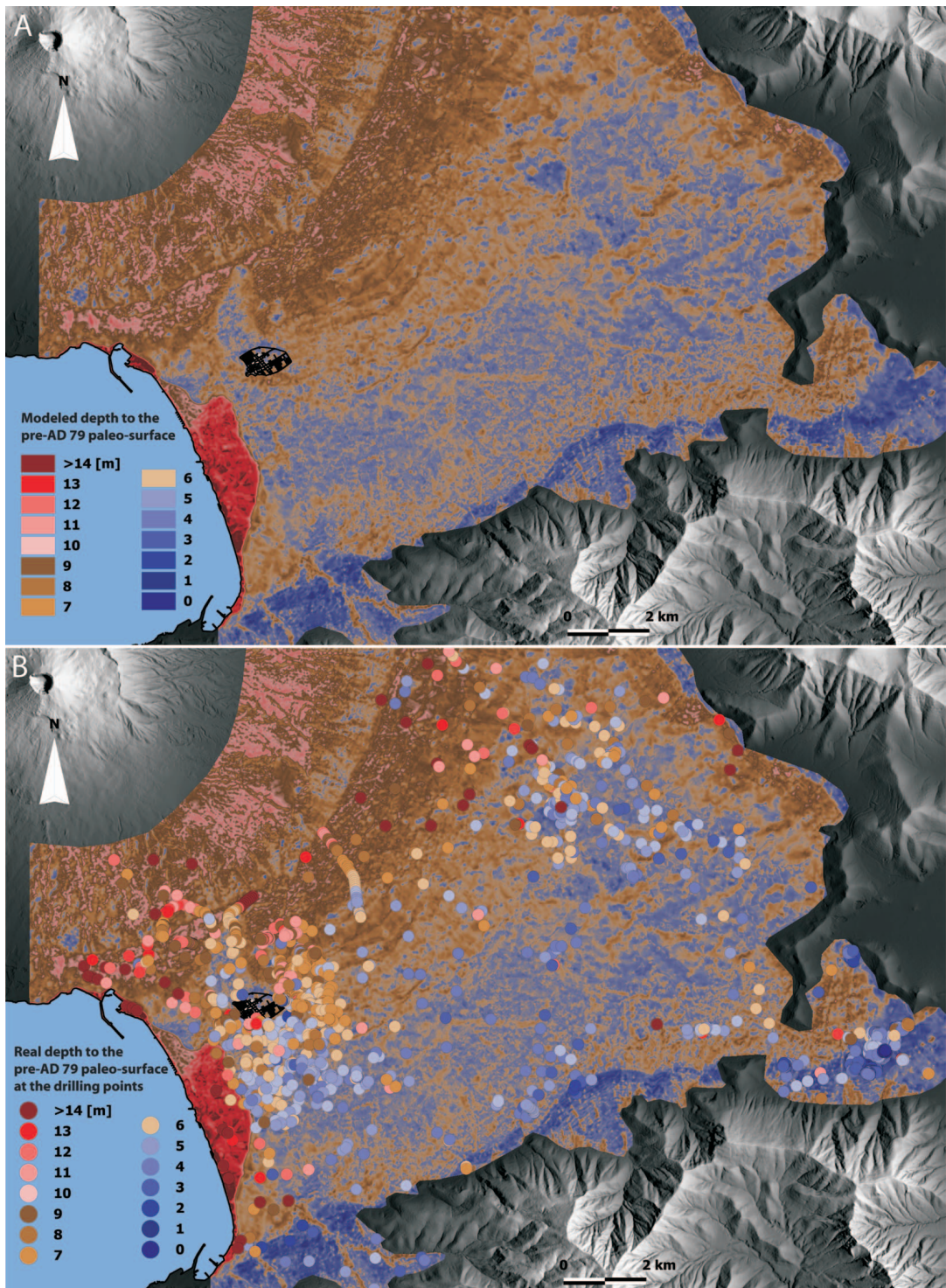


Fig. 4. **A** — Modelled depth to the pre-AD 79 surface (thickness of post-AD 79 deposits) of the Sarno River plain. **B** — Combination with the actual depth to the pre-AD 79 surface at the drilling points.

Table 2: Ranking of importance of the predictor variables used for the model generation.

Variable	Importance [%]
Elevation above sea level	100.0
Aspect	93.1
Channel base level	81.6
Altitude above Channel network	59.0
Slope	52.8
Analytical hillshade	50.6
LS-factor	48.6
Curvature classification	46.7
Convergence index	45.9
Profile curvature	44.3
Topographic wetness index	44.1
Stream power	43.8
Curvature	43.2
Plan curvature	41.9
Catchment area	38.5
Channel network	9.8

distinct spatial distribution of post-AD 79 volcanic deposits is most notably controlled by two sets of processes: (i) the initial deposition of pyroclastic material during the eruption of the Somma-Vesuvius volcanic complex and (ii) the subsequent redistribution of the volcanic material by processes of erosion, transport and redeposition (Vogel & Märker 2010). It is noticeable that within the Sarno River plain there is a gradient of post-AD 79 deposits from the slopes of Somma-Vesuvius in the northwest to the actual plain in the south-east. Thicker deposits on the southwestern slopes of Somma-Vesuvius can be explained as follows (see also Vogel & Märker 2010):

(i) Originating from the vent of Somma-Vesuvius, AD 79 the pumice lapilli fallout was dispersed concentrically towards the southeast resulting in thickest deposits in the perivolcanic areas, near the source of the eruption. This corresponds to isopachs of the thickness of the AD 79 pumice fallout as reconstructed by Sigurdsson & Carey (2002) or Pfeiffer et al. (2005).

(ii) The pumice fallout is overlain by pyroclastic surge and flow deposits of the AD 79 eruption that are especially concentrated at the slopes of Somma-Vesuvius and gradually decrease in thickness towards the plain (Di Vito et al. 1998; Rossano et al. 1998; Di Maio & Pagano 2003). However, along the south-eastern slope of Somma-Vesuvius a band of thinner deposits can be noticed (Fig. 4A) that extends concentrically between 50 and 70 m a.s.l. (present-day elevation). This band may be caused by a downslope acceleration of the pyroclastic surge due to the steepness of the slope temporarily compensating the deceleration of the surge with increasing travel distance. Hence, the erosive power of the surge is temporarily increased before deposition prevails towards the toe-slope of Somma Vesuvius (see Rossano et al. 1998).

(iii) Additionally, the slopes of Somma-Vesuvius are covered by pyroclastic material and lava flows from more recent eruptions such as AD 472, 1631 or 1944 (Geological map 1:10,000, Autorità di Bacino del Sarno 2003).

Greater thickness of volcanic deposits in the coastal area on the other hand can be attributed to mobilization of initially deposited material by the paleo-Sarno River and its tributaries,

transportation out of the plain and finally re-deposition in shallow water along the Tyrrhenian coast. This coincides with rather thin deposits in the central and southern parts of the Sarno River plain. Steep slopes of 3 to 4 m in height near the Tyrrhenian Sea give a first idea on the approximate position of the coastline before AD 79 (Fig. 4A).

An accumulation of deposits on the foot slopes of the Sarno and Lattari Mountains results from initially deposited volcanic material that was eroded by mountain streams or lahars, for example after intense rainfall events (Lirer et al. 2001; Fiorillo & Wilson 2004). Accordingly, the mountain slopes from where this material was eroded show relatively thin post-AD 79 deposits. Likewise, the volcanic material on the Pompeian hill is rather thin on top and thicker along its foot slopes because after the deposition of the AD 79 volcanic material it was eroded from the ridge and accumulated in the adjacent plain.

It is noticeable that on the western slopes of the Lattari Mountains thicker deposits appear within the deeply incised river valleys such as the 'Fosso di Gragnano' draining this part of the mountains whereas the adjacent slopes show rather thin deposits. This is supported by Rossano et al. (1998) who state in the Vesuvius area that the movement and deposition of ash flows, lahars or debris avalanches accompanying volcanic eruptions strongly follow topographic irregularities such as river channels. Furthermore, due to the redistribution of the volcanic material subsequent to the AD 79 eruption paleo-river valleys were filled with volcanic material that was initially deposited on the mountain slopes.

The improved digital elevation model (DEM) of the Sarno River plain before AD 79 was calculated by subtracting the modelled thickness of the post-AD 79 deposits from the present-day surface. The pre-AD 79 paleo-river network was deduced by deriving the linear thalweg features of the pre-AD 79 DEM (Fig. 5). Finally, the reconstruction of specific paleo-environmental features before AD 79 was done by attributing the classified environmental characteristics of the pre-AD 79 layer taken from the drilling data to the pre-AD 79 topography (Fig. 6A). Hence, the approximate course of the coastline before AD 79 and the floodplain of the paleo-Sarno River were delineated by means of the littoral and the fluvial-palustrine environmental information from the drilling data. Marine and littoral deposits that were found inland from the ancient coastline identified the approximate location of the protohistorical dune ridges of Messigno (5,600–4,500 yr BP) and Bottaro/Pioppaino (3,600–2,500 yr BP) (Cinque 1991) (Fig. 6B) (Vogel & Märker 2010).

As Vogel & Märker (2010) have already stated the pre-AD 79 topography corresponds to the present-day topography since the main topographic elements reappear. However, the pre-AD 79 paleo-surface is situated approximately 5.8 m (mean) below the modern surface resulting in a wide area of the Tyrrhenian coast lying below the present-day sea level. The course of the fluvial network before AD 79 and today also have a lot of similarities even though especially the lower reaches of the Sarno River are regulated and canalized today whereas the paleo-Sarno River shows more natural fluvial patterns (Fig. 5). South of Pompeii the paleo-Sarno River flows around the more elevated protohistorical dune ridge of

Messigno and cuts the dune ridge of Bottaro/Pioppaino before it enters the Tyrrhenian Sea about 1.5 km east of the present-day Sarno River (Vogel & Märker 2010) (Fig. 6B).

The general drainage system of the pre-AD 79 Sarno River network can be considered dendritic. The contributing streams follow mainly the slope of the terrain whereas strong structural influences seem to be absent. However, Fig. 7A shows that small segments of the paleo-river network may

also be subject to some kind of structural control as they repeatedly follow right angles that are orientated NE-SW and NW-SE. This would rather suggest a rectangular drainage system. In fact the right angles of the paleo-river network align with the two main fault systems in whose intersection the Sarno River plain is structurally located: (i) that of Somma-Vesuvius volcanic complex which is orientated NE-SW and (ii) that of the Apennines which is NW-SE trending

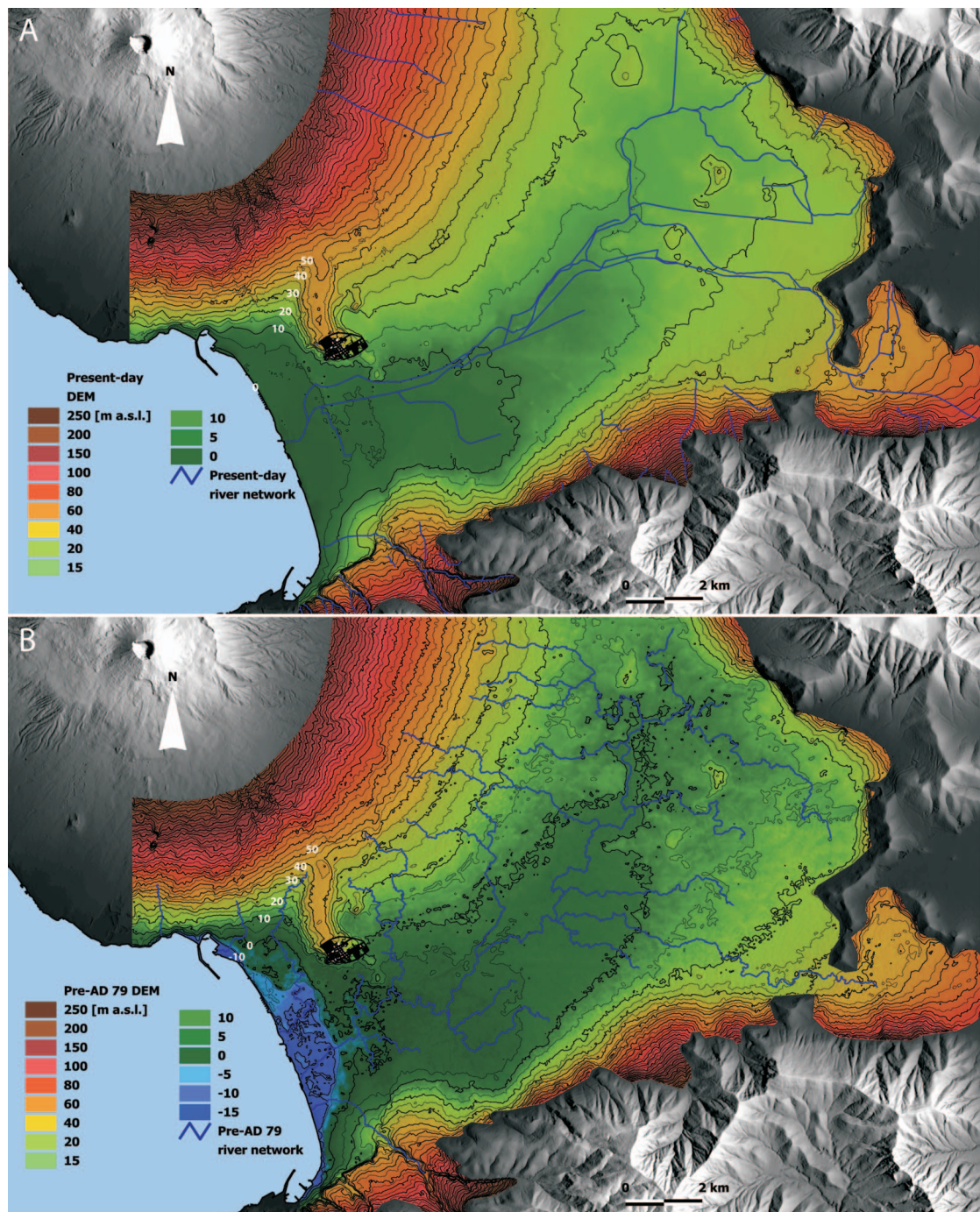


Fig. 5. Present-day (A) and modelled pre-AD 79 digital elevation model (DEM) (B) of the Sarno River plain with fluvial network (A — regulated and canalized present-day Sarno River, B — modelled pre-AD79 Sarno River) and 5 m-contour lines (10 m lines: solid, 5 m lines: thin; white numbers indicate the elevation [m a.s.l.]).

(Del Pezzo et al. 1983; Balducci et al. 1985; Marzocchi et al. 1993; Bianco et al. 1997; Cella et al. 2007). Several hundred seismic events, mostly of volcano-tectonic type, are recorded each year in the Somma-Vesuvius area (Bianco et al. 1997; Del Pezzo et al. 2004). That can probably also be presumed for the time before AD 79. Consequently, seismic events amplify the underlying tectonic structure and thus, partly influence the course of the pre-AD 79 fluvial network. This results in segments of a rectangular drainage system. In contrast,

the river tends to eliminate those structures due to fluvial erosion and accumulation during seismic quiescence which leads to a dendritic drainage system (Fig. 7A).

In the southwest of the Sarno River plain between the Tyrrhenian coast and the Lattari Mountains a big alluvial fan re-emerged on the new pre-AD 79 DEM. This was already identified by Vogel & Märker (2010) and named in the geomorphological map of Cinque (1991) ‘conoide di Muscarello’. In the west there are the much smaller alluvial fans of

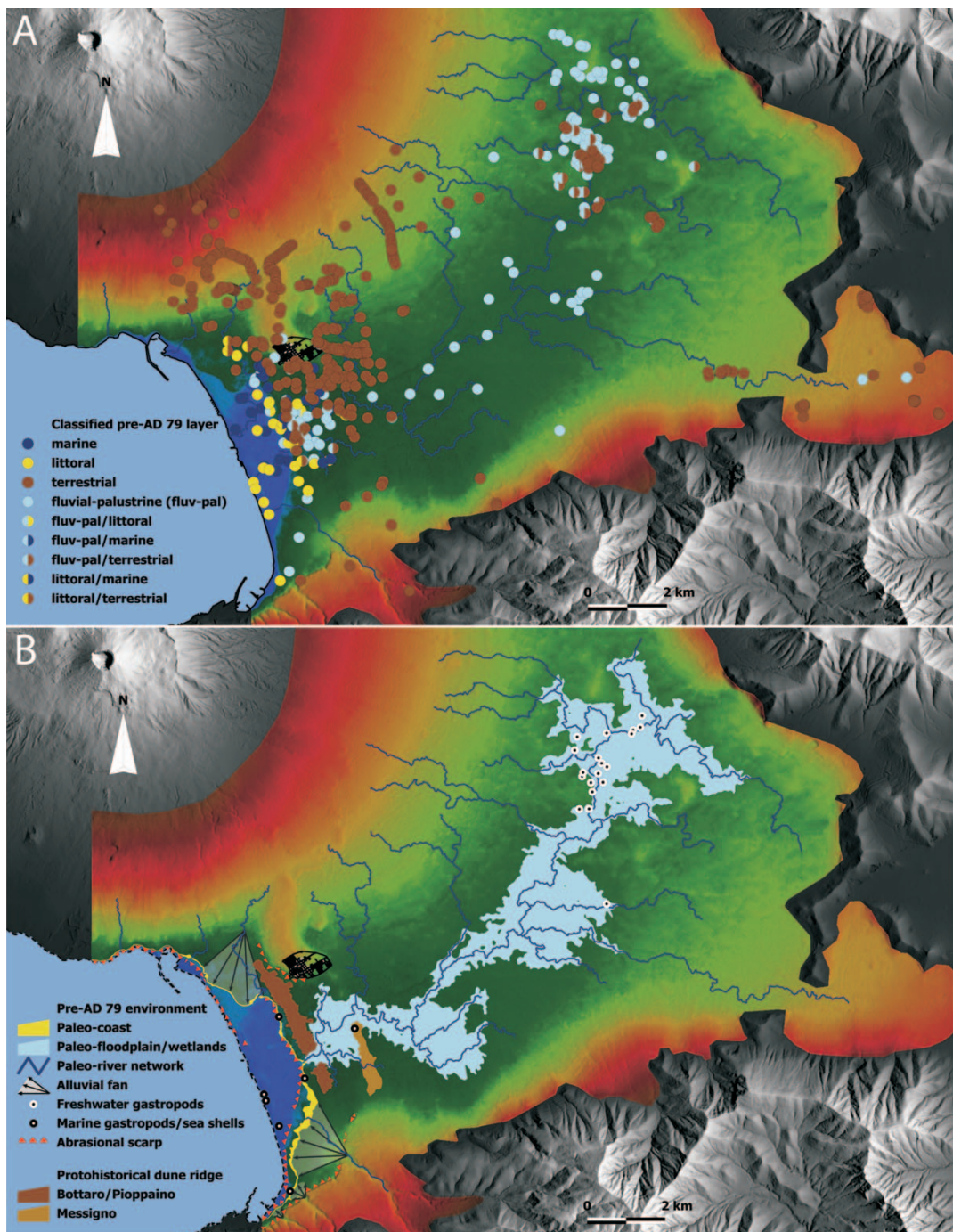


Fig. 6. A — Drilling data on the classified pre-AD 79 layer. B — Inferred reconstruction of pre-AD 79 paleo-environmental and paleo-geo-morphological features.

Sommuzzariello and Quisisana (Cinque 1991) (Fig. 7B). That these alluvial fans already existed before AD 79 is confirmed by Irollo (2005) who determined that the initial deposition of the 'conoide di Muscariello' occurred in the Upper Pleistocene (15–13 ka BP).

Due to the volcanic activity of Somma-Vesuvius and the resulting recurring accumulation of volcanic deposits in that area the coastline of the Sarno River plain continuously propagated westwards (Cinque et al. 1987; Livadie et al. 1990;

Cinque 1991). This is particularly evident in the protohistorical dune ridges of Messigno and Bottaro/Pioppaino that can be found approximately 3,000 m and 1,500 m inland from the present-day coast. Consequently, it can be presumed that during its early formation the 'conoide di Muscariello' extended directly into the Tyrrhenian Sea and was partly deposited underwater. In fact, stratigraphical investigations by Irollo (2005) illustrate both marine/littoral and alluvial deposits suggesting a combination of fluvial and marine deposition.

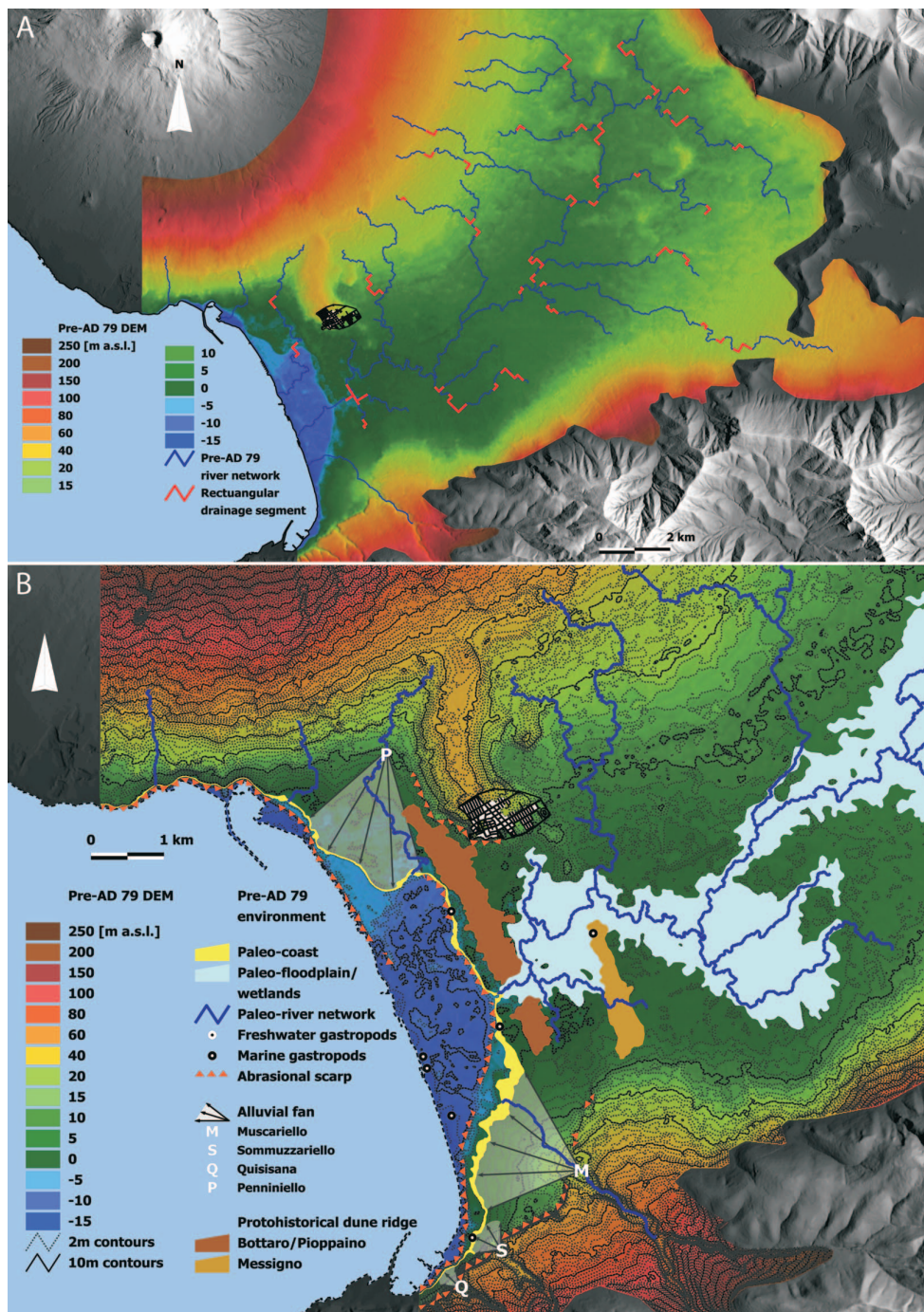


Fig. 7. A — Pre-AD 79 DEM of the Sarno River plain and pre-AD 79 river network. The drainage system can be considered dendritic with scattered rectangular segments that result from structural control (red). B — Paleo-geomorphological map of the Sarno River plain before AD 79.

The paleo-Gragnano River, the main tributary of the ‘conoide di Muscariello’, before AD 79 flowed to the northwest and entered the sea in the north of the alluvial fan (Fig. 5B). The present-day ‘Fosso di Gragnano’ instead flows to the west and into the sea in the very southwest around 1,300 m away from its paleo-mouth before AD 79 (Fig. 5A). The relocation of the river channel might have been caused by the sudden large amount of sediments during the AD 79 eruption of Somma-Vesuvius or subsequent lahars. This may have led to the burial of the paleo-river channel of the ‘Fosso di Gragnano’ and thus to its relocation to the southwest.

Between the western slope of the Pompeian hill and the southern slope of Somma-Vesuvius volcano another alluvial fan was identified which is fed by the main discharge of that area. Cinque (1991) referred to it as ‘conoide di Penniniello’. It is striking that the southwestern, and so presumably youngest part of the fan lies approximately 2 m higher than its central or southeastern part. This accumulation may have been caused by a high sediment load after an eruption of Somma-Vesuvius that eventually forced the river to bend to the south instead of flowing straight to the southwest and directly entering the sea. The contour lines show clearly that the stream has already cut into its own deposits. The northern branch of the protohistorical dune ridge of Bottaro/Pioppaino was most likely dissected by fluvial erosion leaving only scattered traces of dunal deposits (Fig. 7B) due to the morphology of the ‘conoide di Penniniello’.

The pre-AD 79 coastline, prior to the eruption of Somma-Vesuvius, was reconstructed according to the littoral deposits from the drilling data and the pre-AD 79 coastal topography. In its central part the ancient coast runs nearly parallel to the modern coast in a distance of 1,100 to 1,300 m inland. On the slopes of Somma-Vesuvius and the Lattari Mountains the paleo-coast and the modern coast are much closer to each other with distances between 50 and 150 m. Between the mountain slopes and the plain the alluvial fans of Muscariello and Penniniello result in a northwestwards and southwestwards propagation of the ancient coastline, respectively. Regarding the pre-AD 79 topography, the pre-AD 79 coastline is mainly situated between the -2 m and -4 m contour lines in the north near Somma-Vesuvius and between the 0 and 1 m contour line in the south of the plain. This elevation unconformity of the pre-AD 79 littoral deposits can most likely be attributed to some neotectonic activity in the study area. Sigurdsson et al. (1985) and Livadie et al. (1990) also observed a deeper occurrence of the Roman littoral deposits in the north of the Sarno River plain at approximately -4 m a.s.l. which Pescatore et al. (2001) explained with a more rapid subsidence near Somma-Vesuvius in comparison with more distal areas.

Converging contour lines in the coastal area of the Sarno River plain may indicate abrasion terraces that can be related to marine erosion of different coastlines. Abrasional scarps at the foot of the Pompeian hill and the Lattari Mountains derive from protohistorical coastlines (Cinque 1991; Vogel & Märker 2010). Along the pre-AD 79 coastline marine scarps can be found on the slopes of Somma-Vesuvius and in the central part of the coast (Fig. 7B).

Additional marine scarps between the pre-AD 79 and the present-day coastline refer to more recent processes

(Fig. 7B). Due to the modelling approach, post-AD 79 processes have generated those features that are, by mistake, reflected in the pre-AD 79 topography. Consequently, they must be regarded as modelling artefacts. Those terrace features may be formed during post-AD 79 sea levels. As a result of Plinian and sub-Plinian eruptions of Somma-Vesuvius, as in AD 472 or 1631 (Rosi et al. 1993; Rolandi et al. 1998) excessive loads of volcanic sediments were produced that were subsequently redistributed by the river network and redeposited in the coastal area. Finally, this caused a further westward propagation of the coastline.

The floodplain of the paleo-Sarno River was reconstructed by combining the fluvial-palustrine deposits from the drilling data with the pre-AD 79 topography and the deduced pre-AD 79 paleo-river network. As Vogel & Märker (2010) already stated in the previous model the fluvial-palustrine deposits fit very well with the pre-AD 79 paleo-river network (Fig. 6A). They are characterized by the 1 to 2 m isolines of the ‘vertical distance to channel network’ index from the SAGA terrain analysis module (Olaya & Conrad 2008).

Conclusion and outlook

A revised reconstruction of the pre-AD 79 topography of the Sarno River plain was carried out on the basis of an improved classification and regression model of Vogel & Märker (2010). The pre-AD 79 digital elevation model and the classified environmental characteristics of the pre-AD 79 layer derived from the drilling data was used to reconstruct paleo-environmental and paleo-geomorphological features of the Sarno River plain such as the paleo-coastline, the paleo-Sarno River and its floodplain, alluvial fans near the Tyrrhenian Sea as well as abrasion terraces of historical and protohistorical coastlines. However, as already stated by Vogel & Märker (2010) this reconstruction must be considered as a model of the pre-AD 79 conditions based on the hypothesis stated above. Especially neotectonic phenomena that occurred between AD 79 and today are only in part considered in the modelling approach, for example, through the elevation of the pre-AD 79 littoral deposits.

The collection of additional stratigraphical data especially within areas of the Sarno River plain that are insufficiently covered by previous core drillings as well as the combination of the pre-AD 79 DEM with archaeological findings can enhance the paleo-environmental reconstruction of the Sarno River plain.

In the next project phase geomorphologically interesting landforms such as the alluvial fan of ‘Muscariello’ and the floodplain of the paleo-Sarno River will be studied in more detail using geophysical prospections to further verify the pre-AD 79 DEM and the applied methodology. Moreover, the pre-AD 79 DEM and paleo-environment will be utilized to further reconstruct the ancient cultural landscape of the Sarno River plain, for example, the phenomenon of the Roman farms or the ancient road network.

Acknowledgments: This study is part of the geoarchaeological research Project entitled “Reconstruction of the ancient

cultural landscape of the Sarno River plain" undertaken by the German Archaeological Institute in cooperation with the Heidelberg Academy of Sciences and Humanities. It was partly funded by the German Archaeological Institute, Berlin Head Office (Cluster 3) and the Deutsche Forschungsgemeinschaft (German Research Foundation). We would like to thank our local project partners and all their collaborators for their cooperation, particularly the Autorità di Bacino del Sarno, the Soprintendenza Speciale per i Beni Archeologici di Napoli e Pompei, the Soprintendenza per i Beni Archeologici di Salerno e Avellino. We also thank Giovanni Di Maio, Giovanni Patricelli and Gaetana Saccone for various supports. Finally, we would like to thank Angus Duncan, Jiří Šebesta, and Jozef Minář for reviewing and substantially improving the paper with constructive comments and suggestions.

References

Andronico D., Calderoni G., Cioni R., Sbrana A., Sulpizio R. & Santacroce R. 1995: Geological map of Somma-Vesuvius volcano. *Per. Mineral.* 64, 77–78.

Autorità di Bacino del Sarno 2003: Geological map, scale 1: 10,000. *CARG Project*, Region Campania (in Italian).

Balducci S., Vasellini M. & Verdiani G. 1985: Exploration well in the 'Ottaviano' Permit, Italy; 'Trecase 1'. In: Strub A.S. & Ungermaier P. (Eds.): European Geothermal Update. *Proc. 3rd Int. Seminar on the Results of EC Geothermal Energy Research*, Reidel.

Beers T.W., Dress P.E. & Wensel L.C. 1966: Notes and observations. Aspect transformation in site productivity research. *J. Forestry* 64, 691–692.

Bianco F., Castellano M., Milano G., Ventura G. & Vilardo G. 1997: The Somma-Vesuvius stress field induced by regional tectonics: evidences from seismological and mesostructural data. *J. Volcanol. Geotherm. Res.* 82, 199–218.

Breiman L., Friedman J., Olshen R. & Stone C. 1984: Classification and regression trees. *Chapman and Hall*, New York.

Carey S. & Sigurdsson H. 1987: Temporal variations in column height and magma discharge rate during the 79 A.D. eruption of Vesuvius. *Geol. Soc. Amer. Bull.* 99, 303–314.

Cella F., Fedi M., Florio G., Grimaldi M. & Rapolla A. 2007: Shallow structure of the Somma-Vesuvius volcano from 3D inversion of gravity data. *J. Volcanol. Geotherm. Res.* 161, 303–317.

Cioni R., Marianelli P. & Sbrana A. 1992: Dynamics of the A.D. 79 eruption: Stratigraphic, sedimentological and geochemical data on the successions from the Somma-Vesuvius southern and eastern sectors. *Acta Vulcanol.* 2, 109–123.

Cinque A. 1991: The versilian transgression in the Sarno River plain, Campania. *Geogr. Fis. Dinam. Quat.* 14, 63–71 (in Italian).

Civetta L., Galati R. & Santacroce R. 1991: Magma mixing and convective compositional layering within the Vesuvius magma chamber. *B. Volcanol.* 53, 287–300.

Civetta L., Di Vito M.A., De Lucia M. & Isaia R. 1998: Eruptive history of Somma-Vesuvius. In: Guzzo P. & Peroni R. (Eds.): Archeologia e vulcanologia in Campania. *Conference Proceedings, Atti del. Convegno*, Naples, 9–16 (in Italian).

Delibrias G., Di Paola G.M., Rosi M. & Santacroce R. 1979: The eruptive history of Somma-Vesuvius volcanic complex reconstructed from pyroclastic successions of Monte Somma. *Rend. Soc. Ital. Mineral. Petrol.* 35, 411–438 (in Italian).

Del Pezzo E., Iannaccone G., Martini M. & Scarpa R. 1983: The 23 November 1980 southern Italy earthquake. *Bull. Seismol. Soc. Amer.* 73, 187–200.

Del Pezzo E., Bianco F. & Saccorotti G. 2004: Seismic source dynamics at Vesuvius volcano, Italy. *J. Volcanol. Geotherm. Res.* 133, 23–39.

Dikau R. 1988: Entwurf einer geomorphographisch-analytischen Systematik von Reliefeinheiten. *Heidelb. Geogr. Baust.* 5, 1–45.

Di Maio G. & Pagano M. 2003: Considerations on the coast line and the modality of burial of ancient Stabia after the Vesuvian eruption AD 79. *Riv. Studi Pomp.* XIV, 197–245 (in Italian).

Di Vito M.A., Sulpizio R., Zanchetta G. & Calderoni G. 1998: The geology of the South Western Slopes of Somma-Vesuvius, Italy, as inferred by borehole stratigraphies and cores. *Acta Vulcanol.* 10, 2, 383–393.

Fiorillo F. & Wilson R.C. 2004: Rainfall induced debris flows in pyroclastic deposits, Campania (southern Italy). *Engng. Geol.* 75, 263–289.

Irollo G. 2005: The Holocene evolution of the coastal area between Naples and Stabia (Campania) based on geological and archaeological data. *Doctoral Thesis. Faculty of Mathematical, Physical and Natural Science. University of Naples "Federico II"*, 1–414 (in Italian).

Köthe R. & Lehmeier F. 1993: SARA — Ein Programmsystem zur Automatischen Reliefanalyse. *Z. Angew. Geogr.* 4, 11–21.

Lirer L., Munno R., Petrosino P. & Vinci A. 1993: Tephrostratigraphy of the AD79 pyroclastic deposits in perivolcanic areas of Mt. Vesuvio (Italy). *J. Volcanol. Geotherm. Res.* 58, 133–149.

Lirer L., Vinci A., Alberico I., Gifuni T., Bellucci F., Petrosino P. & Tinterri R. 2001: Occurrence of inter-eruption debris flow and hyperconcentrated flood-flow deposits on Vesuvio volcano, Italy. *Sed. Geol.* 139, 151–167.

Lividie C.A., Barra D., Bonaduce G., Brancaccio L., Cinque A., Ortolani F., Pagliuca S. & Russo F. 1990: Geomorphologic, neotectonic and volcanic evolution of the coastal plain of the Sarno River (Campania) related to the settlements before AD 79 eruption. *Pact* 25–13, 237–256 (in Italian).

Luongo G., Perrotta A. & Scarpato C. 2003: Impact of the AD 79 explosive eruption on Pompeii. I. Relations amongst the depositional mechanisms of the pyroclastic products, the framework of the buildings and the associated destructive events. *J. Volcanol. Geotherm. Res.* 126, 201–223.

Marzocchi W., Scandone R. & Mulargia F. 1993: The tectonic setting of Mount Vesuvius and the correlation between its eruptions and the earthquakes of the Southern Apennines. *J. Volcanol. Geotherm. Res.* 58, 27–41.

Myles A., Feudale R., Liu Y., Woody N. & Brown S. 2004: An introduction to decision tree modelling. *J. Chemometr.* 18, 275–285.

Ohlig C.P.J. 2001: De Aquis Pompeiorum. In: De Waele J.A.K.E. & Moermann E.M. (Eds.): *Das Castellum Aquae in Pompeji: Herkunft, Zuleitung und Verteilung des Wassers. Circumvesuviana* 4, 2001, 1–483.

Olaya V. & Conrad O. 2008: Geomorphometry in SAGA. In: Hengl T. & Reuter H.I. (Eds.): *Geomorphometry: concepts, software, applications*. Elsevier, 1–765.

Pescatore T., Senatore M.R., Capretto G. & Lerro G. 2001: Holocene coastal environments near Pompeii before the A.D. 79 eruption of Mount Vesuvius, Italy. *Quat. Res.* 55, 77–85.

Pfeiffer T., Costa A. & Macedonio G. 2005: A model for the numerical simulation of tephra fall deposits. *J. Volcanol. Geotherm. Res.* 140, 273–294.

Roland G., Maraffi S., Petrosino P. & Lirer L. 1993a: The Ottaviano eruption of Somma-Vesuvio 8,000 y B.P. a magmatic alternating fall and flow-forming eruption. *J. Volcanol. Geotherm. Res.* 58, 43–65.

Roland G., Mastrolorenzo G., Barrella A.M. & Borrelli A. 1993b: The Avellino plinian eruption of Somma-Vesuvio 3,760 y B.P. — the progressive evolution from magmatic to hydromagmatic style. *J. Volcanol. Geotherm. Res.* 58, 67–88.

Rolandi G., Petrosino P. & Geehin J. 1998: The interplinian activity at Somma-Vesuvius in the last 3,500 years. *J. Volcanol. Geotherm. Res.* 82, 19–52.

Rosi M., Principe C. & Vecci R. 1993: The 1631 eruption of Vesuvius reconstructed from the review of chronicles and study of deposits. *J. Volcanol. Geotherm. Res.* 58, 151–182.

Rossano S., Mastrolorenzo G. & De Natale G. 1998: Computer simulations of pyroclastic flows on Somma-Vesuvius volcano. *J. Volcanol. Geotherm. Res.* 82, 113–137.

Santacroce R. 1987: Somma-Vesuvius. *C.N.R., Quaderni de 'La Ricerca Scientifica'*, Rome 114, 1–251.

Sigurdsson H., Carey S., Cornell W. & Pescatore T. 1985: The eruption of Vesuvius in A.D. 79. *Natl. Geogr. Res.* 1, 332–387.

Sigurdsson H. 2002: Mount Vesuvius before the Disaster. In: Jaschinski W.F. (Ed.): *The Natural History of Pompeii. Cambridge University Press*, 29–36.

Sigurdsson H. & Carey S. 2002: The Eruption of Vesuvius in A.D. 79. In: Jaschinski W.F. (Ed.): *The Natural History of Pompeii. Cambridge University Press*, 37–64.

Stefani G. & Di Maio G. 2003: Considerations on the coast line of AD 79 and to the ancient port of Pompeii. *Riv. Stud. Pompei XIV*, 142–195 (in Italian).

Vogel S. & Märker M. 2010: Reconstruction the Roman topography and environmental features of the Sarno River plain (Italy) before the AD 79 eruption of Somma-Vesuvius. *Geomorphology* 115, 67–77.

Zevenbergen L.W. & Thorne C.R. 1987: Quantitative analysis of land surface topography. *Earth Surf. Proc. Land.* 12, 47–56.